metals

MDPI

Article

Improved Combustion Performance of Fluororubber-Coated Micro-Nano Composite Aluminum Powder

Xinzhou Wu, Hui Ren * and Qingjie Jiao

State Key Laboratory of Explosion of Science and Technology, Beijing Institute of Technology, Beijing 100081, China
* Correspondence: renhui@bit.edu.cn; Tel.: +86-135-2153-8722

Abstract: In order to improve the reaction rate and reaction degree of aluminized explosives, the micro-nano composite aluminum powder was fabricated by a new method of in situ electro-explosion. The combustion performances of the composite aluminum powder were studied. The results showed that the micro-nano composite aluminum powder was like a "sea urchin structure" with many nano-sized powders around a single micro-sized aluminum particle. The heat of combustion was 25.67 MJ/kg at 3 MPa oxygen pressure, and the rising rate of pressure was particularly obvious. The ignition performance in an air environment was much better than the micro-sized aluminum powder. At the same time, the reaction process of the micro-nano composite aluminum powder was analyzed. The reaction can be divided into three stages, the decomposition of fluororubber between 500 and 600 °C, then melting, and the first step of the oxidation of aluminum powder occurred between 600 and 700 °C. In the third stage, the micro-nano composite aluminum powder reacted violently around 1000 °C and the released energy reached 3779 J/g. The micro-nano composite aluminum powder had excellent combustion performance and a good application prospect in high-power energy storage materials.

Keywords: aluminum powder; combustion performance; micro structure; energy release

Citation: Wu, X.; Ren, H.; Jiao, Q. Improved Combustion Performance of Fluororubber-Coated Micro-Nano Composite Aluminum Powder. *Metals* **2023**, *13*, 556. https://doi.org/10.3390/met13030556

Academic Editor: Kazuyuki Hokamoto

Received: 3 February 2023
Revised: 2 March 2023
Accepted: 8 March 2023
Published: 10 March 2023

1. Introduction

Metal explosives, especially aluminum-containing explosives, take advantage of the high calorific value of aluminum powder (31.8 MJ/kg). Aluminum powder can release a large amount of heat during combustion and thus increase the destructive effect of the explosive [1–4]. However, in the explosion of aluminum-containing explosives, there is a gap between the calculated heat release and the actual measured heat release. The incomplete combustion of aluminum powder is the main reason for the incomplete release of energy [5–8]. Micron-sized aluminum powder has the advantage of a high active aluminum content, but the high ignition temperature and other reasons may make its reaction efficiency somewhat low. In comparison, nano-sized aluminum powder has the advantages of a large specific surface area, more surface active sites, and higher chemical reaction activity [9–11]. There has been a lot of research about nano-sized aluminum powder. Due to the high activity, nano-sized aluminum powder is prone to self-ignition in oxygen-containing environment, and then this ignition will develop into combustion easily, which releases a lot of energy and is difficult to extinguish. Along with that, it easily melts and agglomerates. Agglomeration hinders the reaction, thus reducing the heat released [12,13]. These problems of nano-sized aluminum powder limit the further application in energetic materials. In rare cases where micron- and nano-sized aluminum powders are used together [14,15], it is generally believed that nano-sized aluminum will react faster than the micron-sized aluminum. The burning of micron-sized aluminum will only increase the heat value, which is more reflected in the early reaction of nano-sized aluminum powder to increase the explosive detonation power. The influence of factors

such as the content and microstructure differences between the micro- and nano-sized aluminum powders on the combustion results has not been studied deeply enough.

In order to take advantage of the micron- and nano-sized aluminum powder, the micron-sized aluminum powder and nano-sized aluminum powder were compounded to obtain a special micro-nano composite aluminum powder with high reaction characteristics and better combustion performance. With the high reactivity of nano-sized aluminum powder and the more content of active mass in micron-sized aluminum powder, the reaction rate and reaction efficiency of aluminum powder in explosives are higher, and more and more energy will be released. This paper puts forward the idea that by using nano-sized aluminum and micron-sized aluminum to form a special structure, the special structure looks like a "sea urchin". The use of a nano aluminum powder increases the active sites. Nano aluminum powder reacts quickly, so the special micro-nano composite aluminum powder will react early. When aluminum powders start to release energy, the ambient temperature will rise. On the other hand, the heat of nano aluminum powder combustion release will promote the vaporization of micron aluminum powder. However, in order to solve the problem of agglomeration during the reaction of aluminum powder, the surface of the micro- and nano-sized aluminum powder was coated with a layer of gas-producing material. There was a gas film between each micro-nano composite aluminum powder after the explosive blast, which will hinder agglomeration and increase the degree of dispersion of the active metal powder. To this end, more complete energy is released from the aluminum powders. Fluororubber is widely used as an additive in explosives, aluminum thermite, and other energetic materials. This material has good performance in improving the mechanical safety properties and providing gaseous products such as AlF_3 in the gaseous state and hydrocarbons. Furthermore, many articles have confirmed that fluororubber can enhance the reactivity of aluminum during the reaction [16–18]. Therefore, in this study, a situ electric explosion was used to prepare the sea urchin structure of the nano aluminum-based composite structure. Fixed-volume combustion, laser ignition, thermal analysis, and finite element simulation were used to study the combustion effect of the "sea urchin" structure of the micro-nano-composite aluminum powder. In order to release the energy of the aluminum powder more completely, the reaction mechanism of the composite structure of the nano aluminum powder and the law of the influence of performance will be explored. This is important for the application of aluminum powder in high-power energy storage materials.

2. Materials and Methods

2.1. Materials and Instruments

The Al wire was purchased from Shijiazhuang Zhongli Zinc Industry Company. (Shijiazhuang, China). The heptane (AR) and the ethyl acetate (AR) were both purchased from Chron Chemical Reagent Co., Ltd. (Chengdu, China). The Viton and PTFE were purchased from Liming Research and Design Institute of Chemical Industry Co., Ltd. (Luoyang, China).

An S4800 scanning electron microscope (SEM) (HITACHI, Tokyo, Japan) and Tecnai G2 F30 S-TWIN transmission electron microscope (TEM) (FEI, Hillsboro, USA) were used to observe the shape of the samples. A D8 ADVANCE X-ray diffractometer (XRD) (BRUKER, Billerica, Germany); Thermo ESCALAB 250Xi X-ray photoelectron spectrometer (XPS) (Mosaifei, Waltham, MA, USA) and Vario EL cube elemental analyzer (EDS) (Elementar, Hanau, Germany) were used to analyze the composition of the samples. An ion chromatography (IC) (ICS-1100, Thermo Dionex, Beijing, China) was used to calculate the content of elements such as F.

The reaction mechanism and combustion properties of the samples can be analyzed and described by a TG-DSC simultaneous thermal analyzer, STA 449 F3 Jupiter® (NETZSCH, Selb, Germany); Automatic oxygen bomb calorimeter TRHW-7000C type (Henan Hebi Tianrun Instrument Co. Henan, China); CO_2 laser ignition system ignition device with laser power 50 W (Beijing Keplin Optoelectronics Technology, Beijing, China). A Thousand

Eyes Wolf high-speed camera X113 (Hefei, China) was used to record the ignition and combustion process, with a shooting speed of 6802 frames/s.

2.2. Sample Preparation

The electrical explosion of wire (EEW) is a versatile approach to produce various nanoparticles [19–22]. This method requires a large enough energy and lets the metal wire all vaporize. However, in the electric explosion of the aluminum powder experiments, due to the skin effect of current, the metal wire may not be fully vaporized when the input energy is not quite enough. When the frequency is very high and the current is through the wire, it can be considered that the current flows only in a very thin layer on the surface of the wire, and the center of the wire had almost no current through it. This effect can be described by the following equation.

$$\delta = \sqrt{\frac{2\rho}{\omega\mu}} = \sqrt{\frac{2}{\omega\mu\sigma}} \tag{1}$$

where δ is the skinning depth of the discharge onset; ω is the current angular frequency; μ is the vacuum permeability; ρ is the resistivity of the aluminum wire at room temperature; σ is the specific volume. When the wire is electrically exploded and these products are condensed into particles, the peripheral material is more likely to form smaller-scale particles under the action of high current. Vaporized aluminum condenses on the surface of the micron-sized aluminum, and the special structure consists of micron-size and nano-size aluminum powders.

The sea urchin structure of aluminum nano-based particles was prepared using in situ electro-explosion in an argon environment. In this experiment, the capacitance was kept at 4 μF, the diameter of aluminum wire was 0.6 mm, and the supplied voltage was 14 kV. These collected products were very active and were transferred to heptane to form a slurry. Heptane was very important for preventing the direct oxidation of these active products. First, Viton and PTFE were dissolved in ethyl acetate at 70 °C under ultrasonic agitation until a homogeneous fluororubber solution was formed. Then, the well-dispersed slurry and the products were fully mixed. After the evaporation of the solvent, the resulting mixtures were dried in a vacuum environment at 70 °C for 24 h. The final products were obtained by sifting through a 40-mesh sieve when the solvent was evaporated.

Figure 1a shows the principle of electrical explosion for preparing the micro-nano composite aluminum powder. The material was an aluminum wire that is thicker than the normal aluminum wire used in EEW. The metal vapor was formed during the electrical explosion process, and then the metal vapor condensed into nano-sized aluminum powders and the metal droplets would condense into micron-sized aluminum powders. Figure 1b is the design of the micro-nano composite aluminum powder structure schematic diagram. The center of the micro-nano composite aluminum powder is micron-sized aluminum, nano-sized aluminum is gathered around the micron-sized aluminum, and the surface of the micro-nano composite aluminum powder is coated with a layer of gas-producing material. Fluororubber was chosen due to its stability and combustion properties.

2.3. Experimental Method

The microscopic morphology of the samples was analyzed by scanning electron microscopy (SEM-EDS) and transmission electron microscopy (TEM-EDS). The composition physical and phase analysis were performed by an X-ray diffractometer. The qualitative analysis was performed by an X-ray photoelectron spectrometer and these results helped to determine the composition of the elements as well as the chemical states.

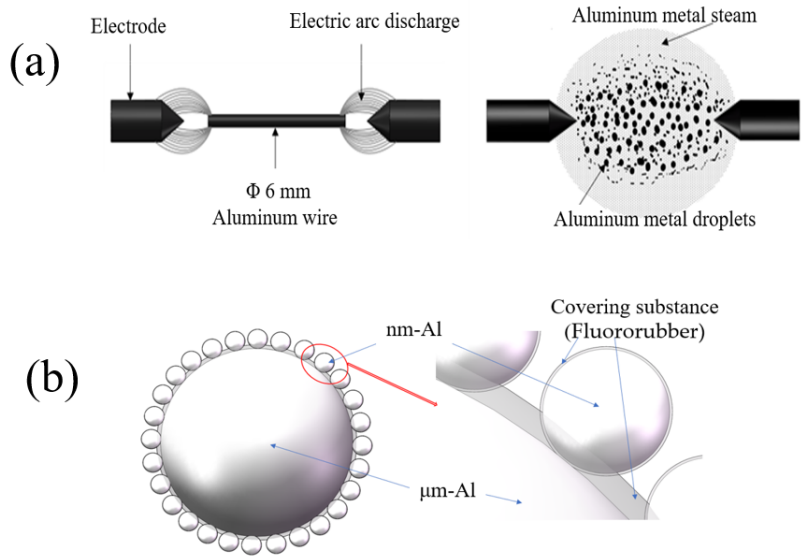

Figure 1. Electric explosion schematic (**a**) and target structure diagram (**b**).

The heat of combustion and pressure results were obtained by using a 330 mL closed oxygen bomb calorimeter. The mass of these samples was 200 mg and the oxygen pressure during the test was 3 MPa. These samples were ignited by the CO_2 laser, and the ignition and combustion were recorded by a high-speed camera. The mass of these samples was 400 mg and the power of the CO_2 laser was 40 W.

The thermal decomposition behavior of the nano aluminum-based composite powder was analyzed under an argon and air atmosphere. Activation energy was calculated with the temperature rise rates of 5 °C/min, 10 °C/min, 15 °C/min, and 20 °C/min, respectively. The Kissinger [23] and Ozawa [24,25] methods were used to estimate the activation energy. The thermal analysis curves of the four temperature rise rates were obtained and the non-isothermal kinetics of the micro-nano-composite aluminum powder was analyzed by calculating the activation energy.

To understand the decomposition process more clearly, the temperature rise of nano-the aluminum-based composite structure was simulated by finite element. The temperature rise simulation and reactivity of the aluminum powder were analyzed. The heat transfer performance of aluminum powder with different structures was studied.

3. Results and Discussion

3.1. Micro-Nano Composite Aluminum Powder Morphology Structure

The SEM images of the micro-nano composite aluminum powder are shown in Figure 2. In this SEM test, a very small amount of spherical aluminum powder was placed on the conductive glue of the sample stage. Figure 2a–c shows photos that have been magnified 400, 10 k, and 60 k times. Many spherical powders can be seen in Figure 2a. Figure 2b,c show spherical powders and a surface with larger magnification. From Figure 2b,c, many nanoparticles were distributed on the 5 μm aluminum surface. Figure 2d shows the micro-nano composite aluminum powder. Figure 2e shows the distribution of element Al, and Figure 2f shows the distribution of element F. Element F in Figure 2f may be not very obvious to see, but the quantitative analysis can be clearly seen in Figure 2g.

In order to see the surface of the particles more clearly, TEM figures of the micro-nano composite aluminum powder are shown in Figure 3. The composite aluminum powder was impregnated in epoxy resin first, and then was sliced into pieces. Around the surface of the micro-nano composite aluminum powder, thin films of about 100 nm and 6 nm existed, respectively. It is presumed that most of these films are fluororubber, and contain small amounts of Al_2O_3 or AlF_3. In Figure 3e, elements Al, O, and F can be seen at the edge of the micro-nano composite aluminum powder.

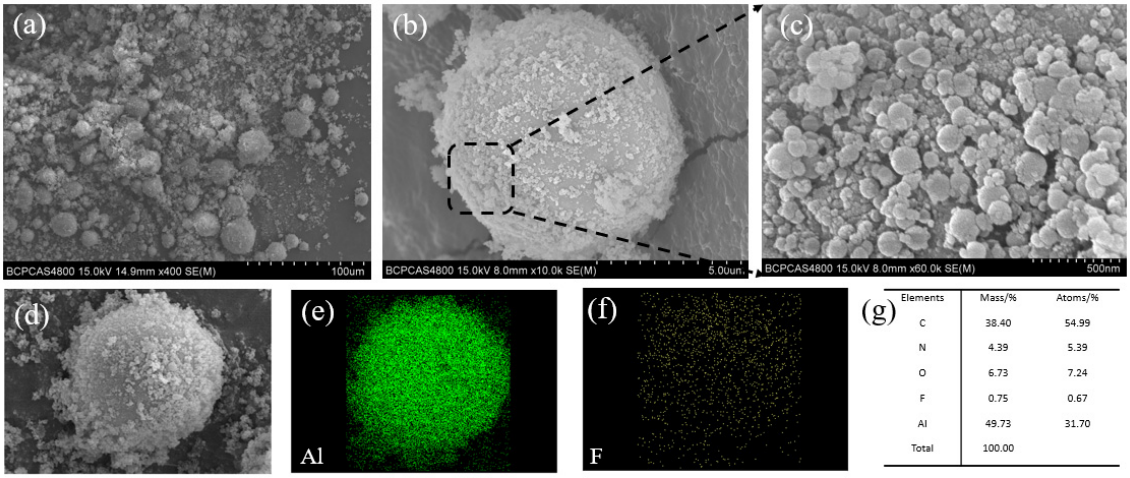

Figure 2. SEM and EDS of the micro-nano composite aluminum powder, micro structure from (**a**–**d**), and element distribution from (**e**–**g**).

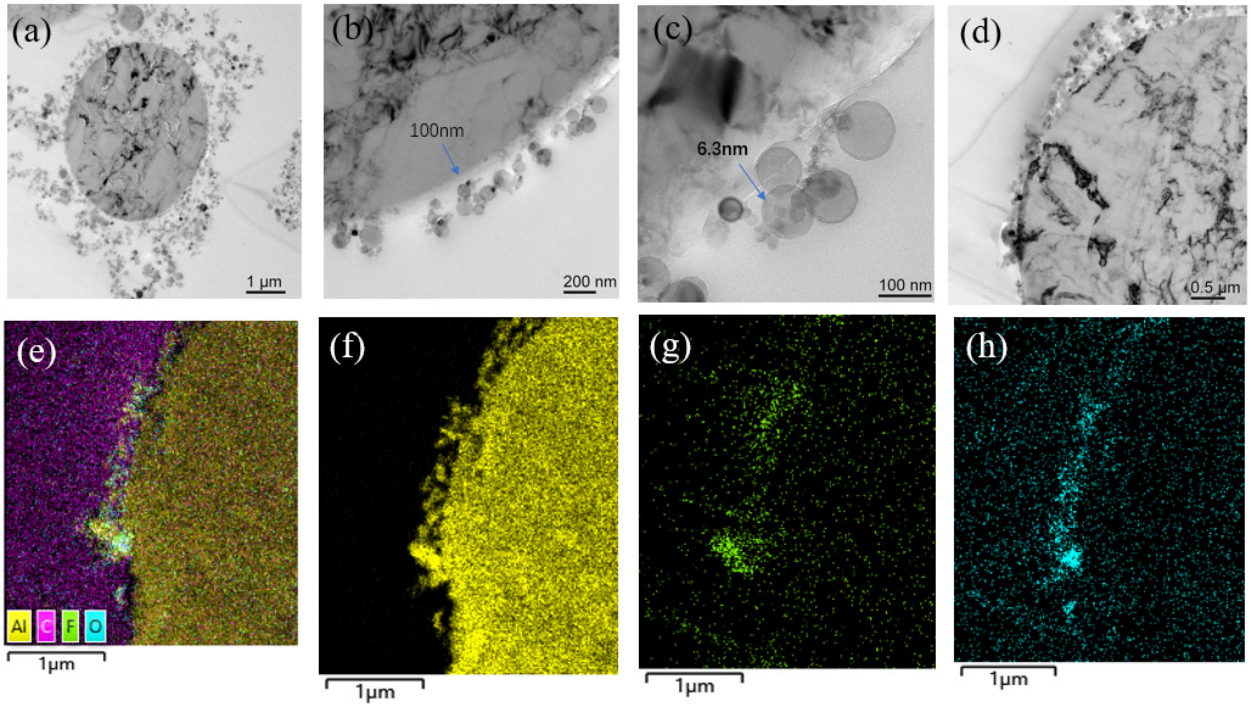

Figure 3. TEM and EDS of the micro-nano composite aluminum powder, micro structure from (**a**–**d**), and element distribution from (**e**–**h**).

The micro-nano composite structure was observed by SEM and TEM, and the nano aluminum spheres were distributed at the edges of the micron aluminum spheres, forming a sea urchin structure with nano aluminum on the outside and a micron-sized aluminum in the middle. From the results in Figure 3, it can be found that the fluororubber was distributed on the surface of the micro-nano composite aluminum powder. Element F is distributed on the surface of the sea urchin structure, which is at the edges of the nano aluminum and micron aluminum. Although the nano parts had different particle sizes and were slightly agglomerated, the micro-nano composite aluminum powder as a whole showed a structure where the micron-sized aluminum spheres were wrapped by nano-sized aluminum spheres.

The oxygen bomb IC results show that the percentage of element F was 7.24%. The calculation obtained that the percentage of fluororubber in the sample was 9.53%, which

was closer to the feeding ratio of 10% fluororubber. It is believed that PTFE and Viton have good uniform mixing in these samples.

The XRD analysis of the micro-nano composite aluminum powder is shown in Figure 4. Only metallic aluminum could be found, and the possible presence of alumina, aluminum fluoride, and other substances were not obvious in this XRD result due to the low content or they were amorphous. Meanwhile, this can also indicate that not many impurities were introduced during the preparation of the sample.

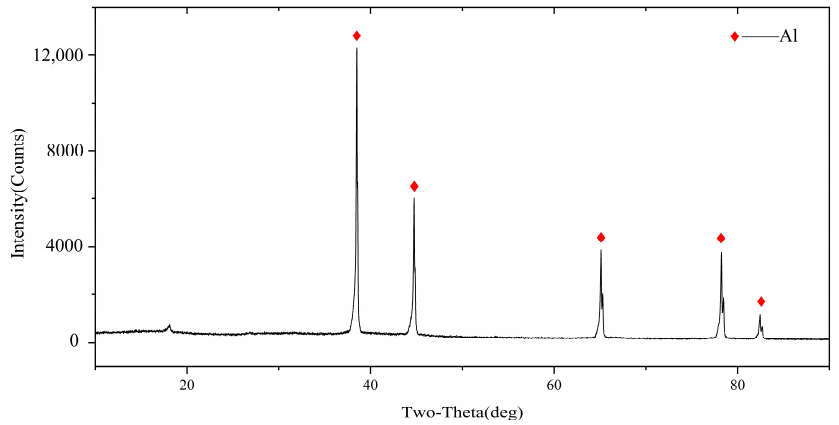

Figure 4. XRD of the micro-nano composite aluminum powder.

The XPS result is shown in Figure 5. Through XPS analysis and splitting the Al2p peak in Figure 5b and the F1s peak in Figure 5c, there were some new components aside from alumina. Two characteristic peaks of element Al at 72.04 eV and 74.38 eV were found, corresponding to metallic Al and 3-valent Al, respectively. There were two oscillatory peaks of element F at 685.48 eV and 689.40 eV, corresponding to AlF_3 and fluororubber, respectively. This indicates that AlF_3 was generated on the surface of the aluminum spheres, and the adsorption mode between the cladding layer and aluminum powder included chemisorption.

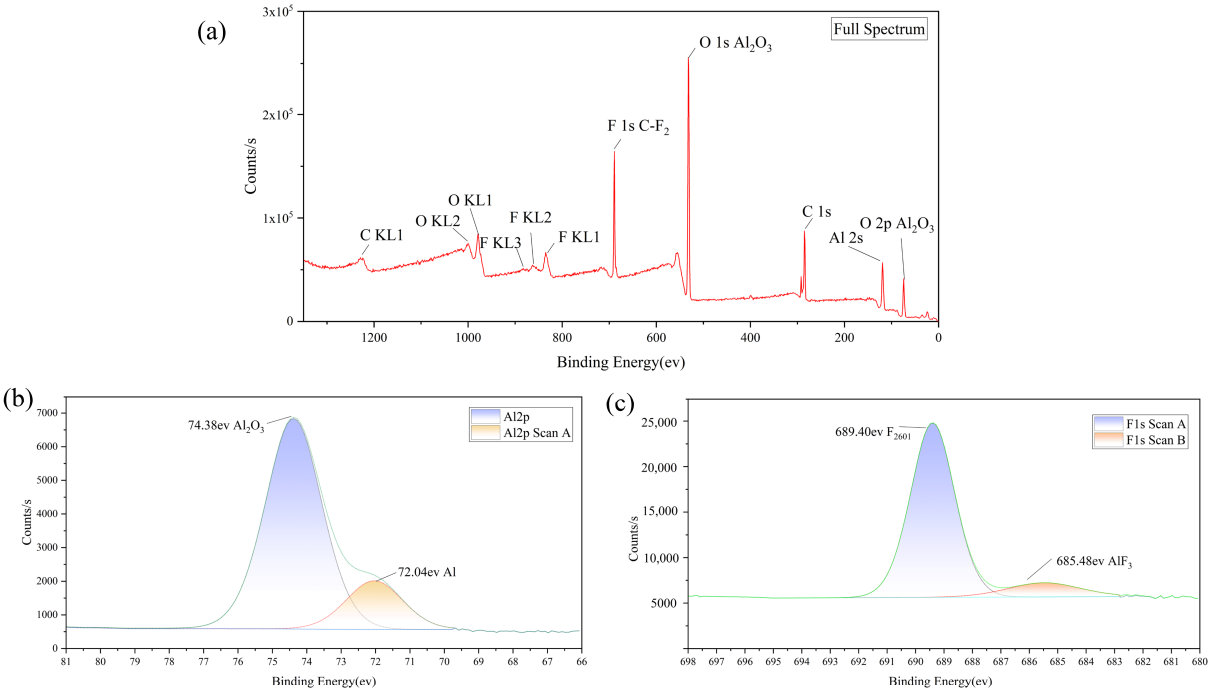

Figure 5. XPS of the micro-nano composite aluminum powder. The full spectrum (**a**), the element Al (**b**), and the element F (**c**).

3.2. Combustion and Ignition Performance

The heat of combustion measurement of the micro-nano composite aluminum powder was 25.67 MJ/kg, which is intermediate between the micron-sized aluminum and nano-sized aluminum, but the *P*–*t* (pressure–time) data results in Figure 6 show that this composite powder had a strong ability to increase the pressure of shockwaves, and the capacity to act and destroy was more reliable. The rate of increase in pressure was 791.41 MPa/s, the difference in pressure (ΔP) was nearly 4 MPa, and the unit impulse (I) could reach 18.8 MPa·s. The micro-nano composite aluminum powder reacted extremely rapidly, and the cladding layer produced gas and dispersed the aluminum powder better.

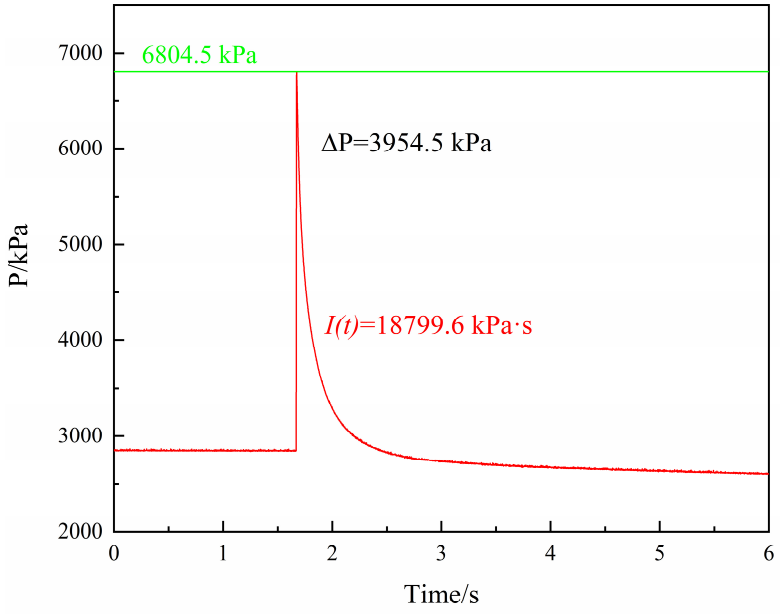

Figure 6. *P*–*t* profiles of samples at a constant volume of 330 mL.

Laser ignition testing is commonly used to characterize the combustion performance of metal powders, and is generally judged by the ignition delay time, radiation intensity, and burning time [26–28]. The laser ignition schematic is shown in Figure 7. The mass of these samples was 400 mg, and was placed at the center of the stage. The shape of the sample was similar to a cone.

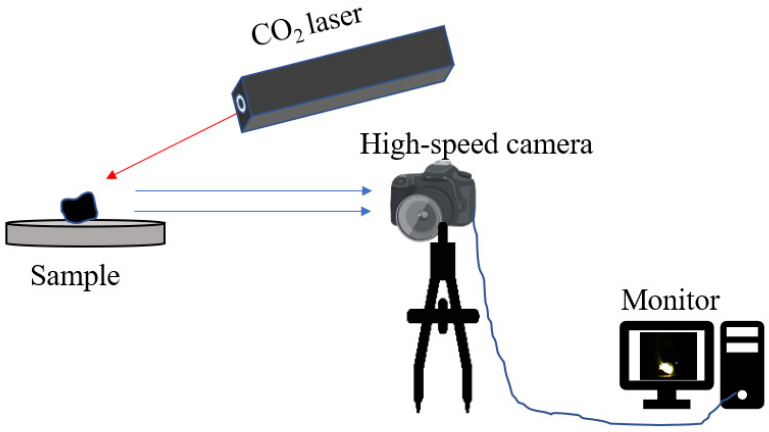

Figure 7. The CO_2 laser ignition schematic.

Comparing the combustion effect of the micro-nano composite aluminum powder and micron-sized aluminum by CO_2 laser ignition in the air condition, it was found that

the micron-sized aluminum could not be ignited under the protection of the aluminum oxide shell. The heat was concentrated in the local area and would not spread.

According to ignition theory, the laser is applied to the surface of the samples. When the energy accumulates at the ignition point of the particles, the particles will ignite and burn. The combustion can be sustained when the net heat (including the exothermic heat of chemical reaction) is greater than the lost heat. For the micro-nano composite aluminum powder, under the hot spot stimulation of the laser, the self-sustained combustion occurred with a faster reaction and more exotherm, which showed a better combustion effect.

The burning effect of aluminum powders was recorded by the high-speed camera in Figure 8. After deducting the background intensity, the combustion intensity of the micro-nano composite aluminum powder was processed, and the results were as follows. The ignition delay time was defined as the point where the radiation intensity suddenly rises, and this moment for the micro-nano composite aluminum powder was in X 5, while the time was about 3 ms. The peak of combustion appeared in X 106, 294 ms from the ignition time; and the burning time was 1.317 s. From Figure 8, the overall radiation intensity showed a trend of first rising and then decreasing. However, the process fluctuated, especially X 302, where the intensity rose at the moment of 885 ms. This was because of the decomposition of fluororubber and the combustion of the nano aluminum powder. The released heat and gas production make the unreacted micro-nano-composite powder fly away and burn violently in the air. It also indicates that the micro-nano composite aluminum powder solves the agglomeration phenomenon during the combustion of micron-sized aluminum powder.

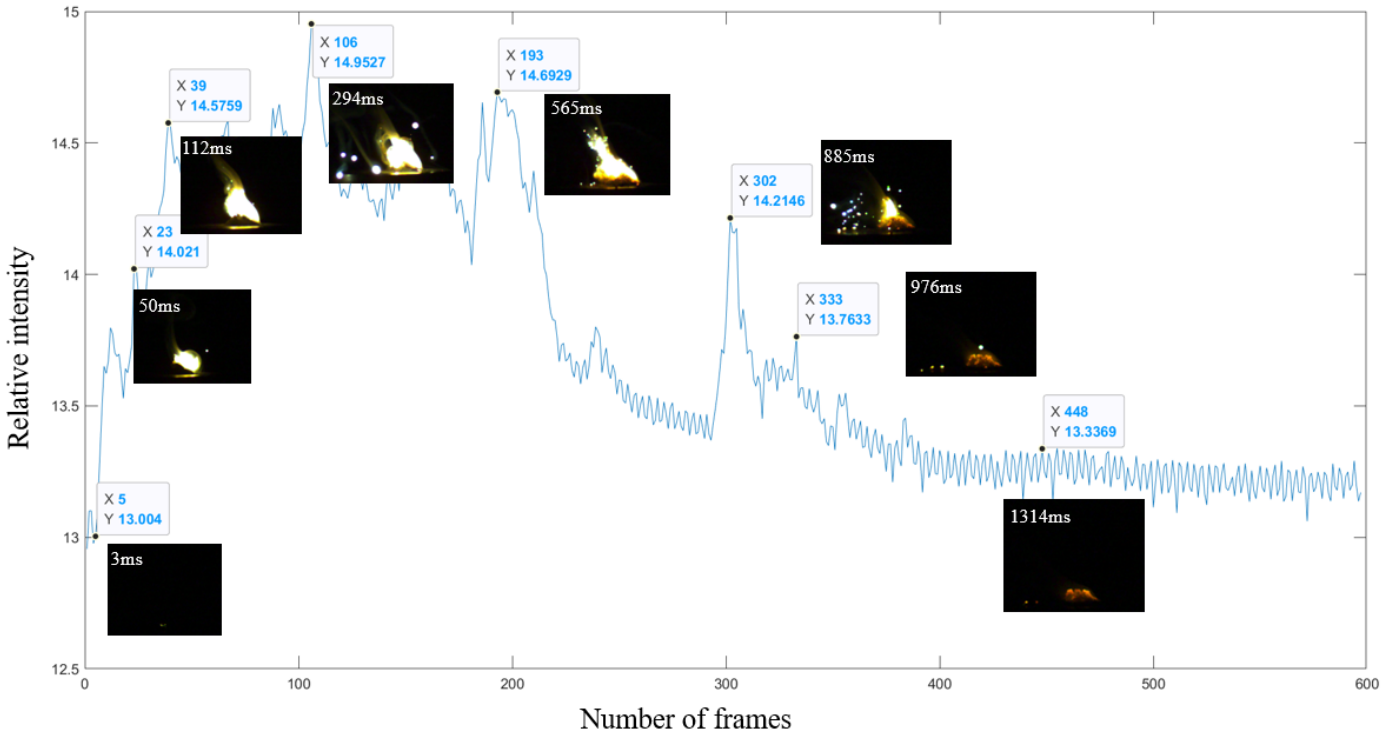

Figure 8. The combustion process of the micro-nano composite aluminum powder.

3.3. Decomposition History

Non-isothermal heating is a very important approach to study the mechanism of decomposition for most substances. The micro-nano composite aluminum powder was heated by the method of TG-DSC under an argon and air atmosphere.

The result at a temperature rise rate of 20 °C/min in an argon atmosphere is shown in Figure 9, and the result in the air atmosphere is shown in Figure 10.

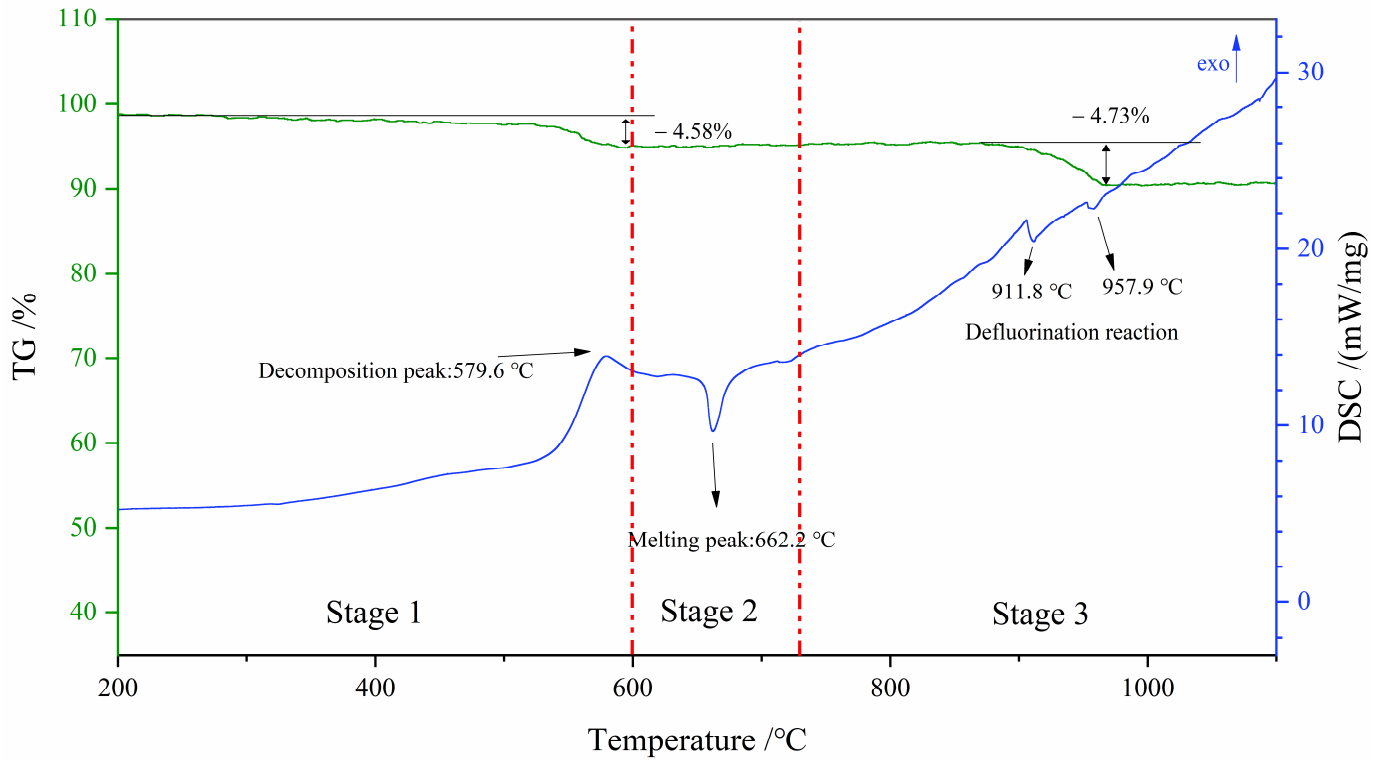

Figure 9. The TG-DSC results of the micro-nano composite aluminum powder in an argon atmosphere at 20 °C/min.

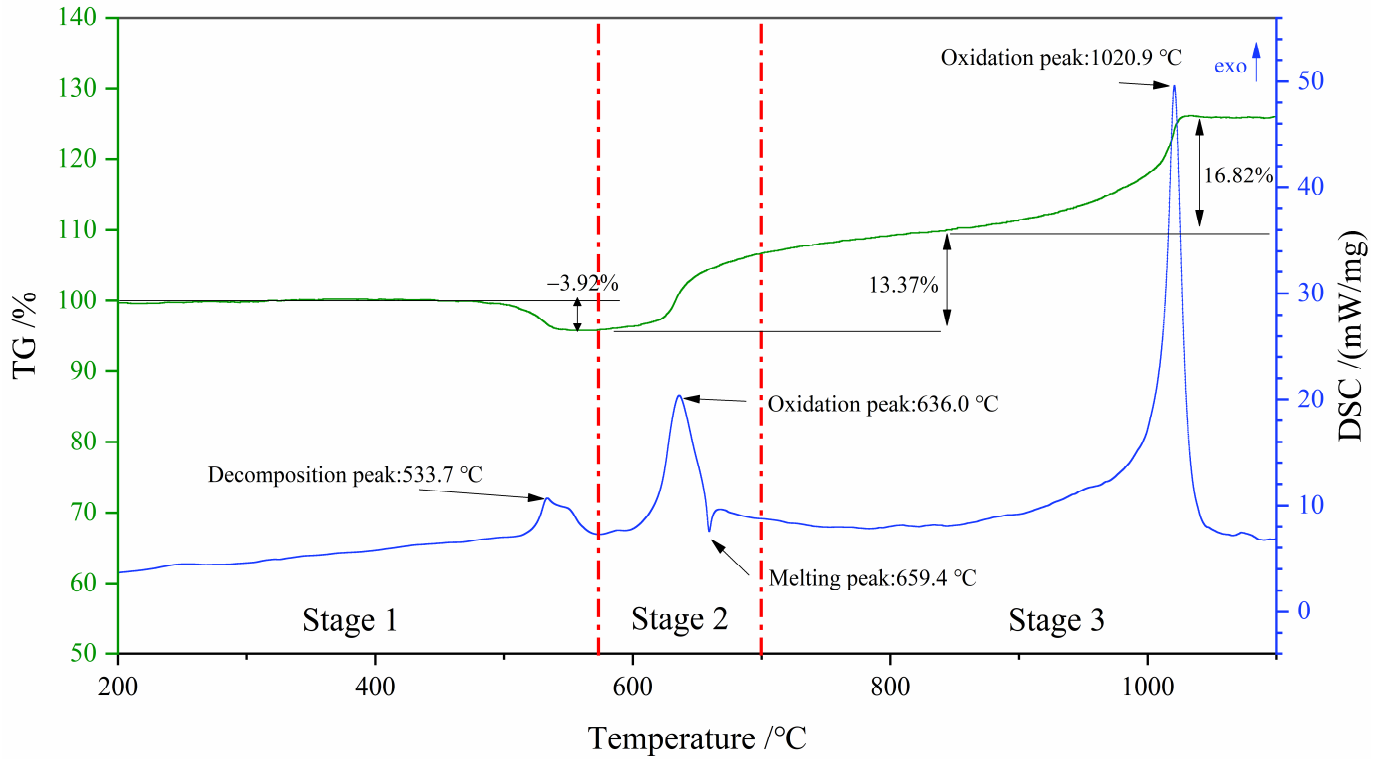

Figure 10. The TG-DSC results of the micro-nano composite aluminum powder in an air atmosphere at 20 °C/min.

The reaction of the micro-nano composite powder can be divided into three stages. The first stage is the decomposition of fluororubber by heat, as shown in Formulas (2)–(4). Meanwhile, the surface of the nano aluminum powder and part of the micron aluminum powder

start to react with the decomposition products of fluororubber, as shown in Formula (5). CO_n stands for CO, CO_2, or a mixture of the two.

$$(-C_2F_4-) \rightarrow CF_2 \quad (2)$$

$$(-C_2F_4-) \rightarrow CF_3 + CF + CF_2 \quad (3)$$

$$CF_3 + CF \rightarrow CF_2 \quad (4)$$

$$Al + Al_2O_3 + CF_2 \rightarrow a(CF_3 + CF) + b(Al_4C_3 + CO_n) + c(AlF3 + C) \quad (5)$$

From Formulas (2)–(5), the turnkey responses can be shown in Formulas (6) and (7).

$$4Al + 3(-C_2F_4-) \rightarrow 4AlF_3 + 6C \quad (6)$$

$$6Al + Al_2O_3 + 3(-C_2F_4-) \rightarrow 4AlF_3 + Al_4C_3 + 2C + CO_n \quad (7)$$

As shown in Figure 9, the second stage had almost no change in mass, and the micro-nano composite aluminum powder melted at about 660 °C. The third stage started to lose weight significantly from about 900 °C, and the defluorination reaction [29] mainly occurred at this stage. These are shown in Formula (8).

$$\begin{aligned} AlF_3 &\overset{Al_2O_3}{\rightarrow} 3F_O^* + Al_{Al} + V_{Al}''' \\ 2AlF_3 &\overset{Al_2O_3}{\rightarrow} 3F_O^* + 2Al_{Al} + 3F' \end{aligned} \quad (8)$$

As a metallic fuel, aluminum powder is usually used to react with air. The TG-DSC results in an air atmosphere is shown in Figure 10. Compared with the argon atmosphere, the decomposition temperature and melting temperature of the micro- and nano-composite powders were slightly advanced. In addition to the above reactions, the common two-step oxidation peaks of aluminum powder appeared before 636.0 °C and 1020.9 °C, respectively. The heat absorption in the second stage of aluminum powder during melting was reduced compared with the argon environment. On one hand, part of the aluminum powder was oxidized around 636.0 °C and the active aluminum content was reduced; on the other hand, the exotherm from the aluminum powder oxidation offset part of the melting heat. In the third stage, a sharp exothermic peak could be seen, and the aluminum powder showed a weight gain of more than 16.82% in this stage. The integration obtained an exothermic heat of 3779 J/g with a violent oxidation reaction.

By calculating the activation energy of the two-step reaction of aluminum powder, the information in Table 1 was obtained. Compared with the micron-sized aluminum, the activation energy calculated of the micro-nano composite aluminum powder by both two methods exceeded that of the micron-sized aluminum. This indicates that the thermal stability of the micro-nano composite aluminum powder may be improved by covering the aluminum powder with fluororubber through chemical adsorption. G(*a*) is the integral model function, and the kinetic mechanism of the product formation for the micro-nano composite aluminum powder is the "Mampel Power" theory, n = 1. Furthermore, in "Mampel Power" theory, n = 3/2 is more suitable for the micron-sized aluminum powder. "n" is the reaction order, and "α" is the degree of reaction.

In terms of the sharpness of the peaks and the amount of heat released, the performance of the micron-sized aluminum powder was poor. The amount of heat released by the micron-sized aluminum powder in this temperature interval was less than that of the micro-nano composite aluminum powder, which exerted 910.8 J/g and 3779.0 J/g in the two steps of oxidation, respectively. The rate of energy release qA much less than that of the latter, which indicated that the aluminum powder surface was exposed after the decomposition of fluororubber, and the rest of the micro-nano composite aluminum powder was oxidized rapidly at high temperature. This makes the growth rate of γ-Al_2O_3 accelerate, the conversion degree deepen, and the heat release rate increase.

Table 1. The calculation result of the activation energy of the two-step oxidation reaction.

The Micro-Nano Composite Aluminum Powder	**Step 1**	**G (*a*)** $\frac{d\alpha}{dt}$	**Step 2**	**G (*a*)** $\frac{d\alpha}{dt}$
Peak temperature/°C (5, 10, 15, 20 °C/min)	610.6, 623.7, 625.7, 636.0	a (n = 1)	988.0, 1000.2, 1010.5, 1020.9	a (n = 1)
Kissinger (kJ/mol)	359.482	$\frac{d\alpha}{dt} = 10^{29.55} e^{\frac{-372.99}{RT}}$	551.116	$\frac{d\alpha}{dt} = 10^{30.69} e^{\frac{-619.48}{RT}}$
Ozawa (kJ/mol)	356.013		544.276	
The Micron-Sized Aluminum Powder	**Step 1**	**G (*a*)** $\frac{d\alpha}{dt}$	**Step 2**	**G (*a*)** $\frac{d\alpha}{dt}$
Peak temperature/°C (5, 10, 15, 20 °C/min)	588.6, 606.3, 615.2, 622.6	$a^{3/2}$ (n = 3/2)	996.9, 1021.0, 1038.0, 1047.1	$a^{3/2}$ (n = 3/2)
Kissinger (kJ/mol)	248.129	$\frac{d\alpha}{dt} = \frac{2}{3} 10^{18.93} e^{\frac{-247.32}{RT}} a^{-\frac{1}{2}}$	357.653	$\frac{d\alpha}{dt} = \frac{2}{3} 10^{14.52} e^{\frac{-328.83}{RT}} a^{-\frac{1}{2}}$
Ozawa (kJ/mol)	249.836		360.572	

3.4. Temperature Rise Simulation and Reaction History of Micro-Nano Composite Aluminum Powder

The surface of the micro and nano aluminum powder was coated with a layer of gas-producing material, and this method improved the combustion performance according to the experiments. As shown in Table 2, there were thermal performance parameters of fluororubber, aluminum, and alumina. P is the density, Cp is the constant pressure heat capacity, k is the heat conductivity, T1 is the melting point, and T2 is the boiling point. Fluororubber decomposes at about 773 K.

Table 2. The thermal performance parameters.

Materials	**p (kg/m^3)**	**Cp (J/(kg·K)**	**K (J/(kg·K))**	**T1 (K)**	**T2 (K)**
Aluminum	2700	900	238	933	2773
Alumina	3900	857	27	2327	3255
Fluororubber	1850	840	0.13	—	—

Due to the high thermal conductivity of alumina, the aluminum inside will be heated up quickly. In order to simulate the temperature rise of the aluminum powder under the blast environment, the calculation was carried out by building a finite element model. Putting the aluminum particles with the sea urchin structure into the field of 3000 K, Figure 11a shows the established sea urchin structure model and the observation points. When the aluminum ball was heated for 1 ns, the external nano aluminum quickly reached 3000 K while the micron-sized aluminum center remained at room temperature. With some assumptions, only the heat transfer at the boundary was considered. The two-dimensional transient heat transfer equations are written as:

$$\rho C_p \frac{\partial T}{\partial t} + \nabla \cdot \mathbf{q} = Q \tag{9}$$

$$\mathbf{q} = -k \nabla T \tag{10}$$

where $\mathbf{q}$ is the density of heat flow and Q is determined by T_0 = 3000 K in the boundaries.

Figure 11b shows the temperature of the micro-nano composite aluminum powder covered with alumina, and Figure 11c shows the temperature of the fluororubber. It can be seen that the alumina shell will heat up rapidly, but the internal aluminum still has difficulty reacting in time due to the high melting and boiling point of alumina, which makes it difficult to establish an effective oxygen channel. The low decomposition temperature of the polymer itself, and its thermal conductivity and thermal diffusion coefficient are very low, so it is easy to form heat accumulation. Fluororubber can reach the decomposition point at a very fast rate when it is placed in a high temperature environment such as a blast, and it will rapidly crack or decompose, thus exposing the aluminum core.

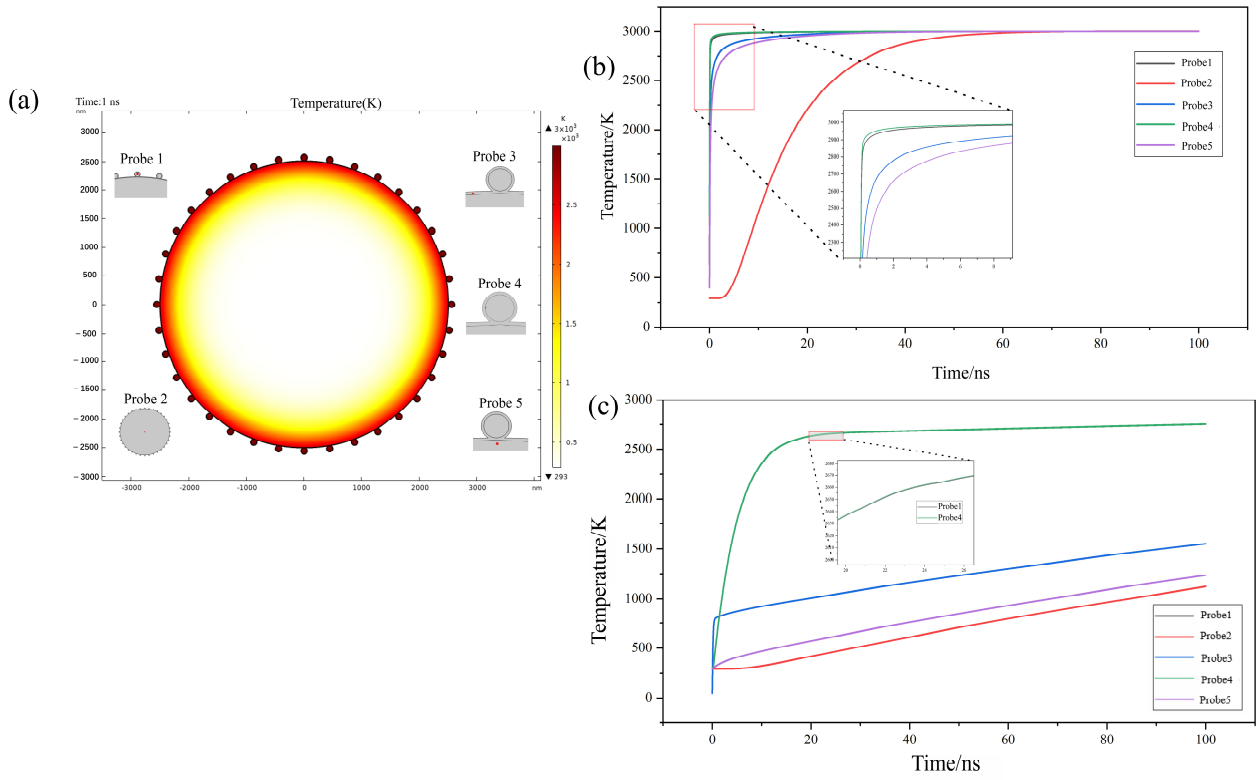

Figure 11. The temperature rise in the micro-nano composite aluminum powder (**a**), the result covered with alumina (**b**), and that covered with fluororubber (**c**).

Considering the differences in the micron-sized aluminum powder and the micro-nano composite aluminum powder, the reactivity of the two powders was calculated. Some assumptions need to be made during the calculation. The main thing is to keep the ambient temperature constant during the burn of micron-sized aluminum powder, and the reaction rate of aluminum powder is mainly determined by the gasification rate [30]. Some assumptions were made to simplify this model. The aluminum particles started burning in the form of a gas-phase reaction, and the reaction rate of aluminum powder was mainly determined by the gasification rate. The gas-phase reaction is so fast that the burning reaction will complete immediately, once the aluminum powder is vaporized. Therefore, the enthalpy of gasification (Ev) was taken from Boltzmann's law.

The system temperature was 4000 K (T_0), the diameter of the micron-sized aluminum powder was 5 µm, and the diameter of the nano aluminum powder was 100 nm. the reaction degree is described by Equations (11) and (12).

$$w = 1 - (1 - \frac{\sqrt{3mkT}e^{-E_v/RT}t}{\pi r^3 \rho x})^3 \quad (11)$$

$$\frac{dw}{dt} = \frac{3\sqrt{3mkT}e^{-E_v/RT}}{\pi r^3 \rho x}(1-w)^{\frac{2}{3}} \quad (12)$$

where w is the mass fraction of the gasification of aluminum particles, and it is also the reactivity. m is the mass of each aluminum atom with a value of 4.48×10^{-26} g. k is Boltzmann's constant, $k = 1.38 \times 10^{-23}$ J/K. T is the temperature, Ev is the enthalpy of gasification, R is the universal gas constant where R = 8.314 J/mol·K. r is the radius of the molecule, and ρ is the density. x is the diameter of the spherical aluminum powder.

According to the results of Figures 2 and 3, the content of the nano aluminum was defined as 8%. At this time, the nano aluminum only covered the surface of the 5 µm aluminum. Nano-sized aluminum reacted much faster than the micron-sized aluminum,

and after the 8% nano-sized aluminum reaction, the remaining micron-sized aluminum reacted at a higher temperature. By calculating the exothermic combustion of the aluminum powder, the temperature would increase by around 475 K (ΔT) at the end of the combustion of 8% nano-sized aluminum The reaction temperature of the remaining micron aluminum was defined as $T_1 = T_0 + \Delta T = 4475$ K. The results of the micron-sized aluminum and the micro-nano composite aluminum powder are shown in Figure 12.

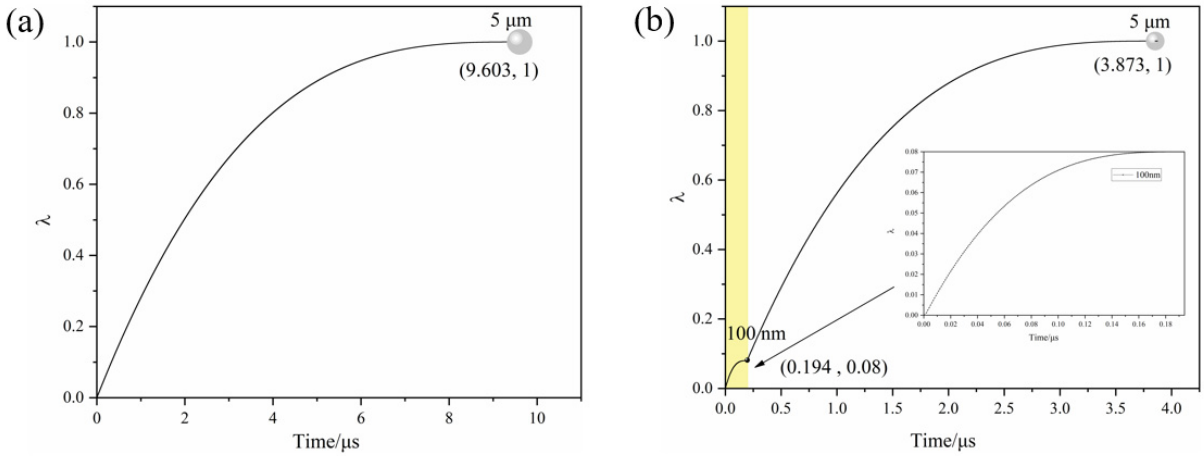

Figure 12. The reaction degree calculation results of the micron-sized aluminum powder (**a**) and the micro-nano composite aluminum powder (**b**).

As shown in Figure 12, the complete reaction time of 5 μm aluminum was 9.603 μs. The reaction of the micro-nano composite aluminum powder was faster and the time was 3.873 μs. The micron-nano composite aluminum took less time to finish the reaction. The micro-nano composite aluminum powder reacted with the explosive in three steps: first, the outer layer of fluororubber will decompose in advance to establish oxygen channels for the internal aluminum nucleus. Then, the nano aluminum powder reacted with air or the fluororubber decomposition products before the micron-sized aluminum due to the size effect and distribution at the periphery of the micron-sized aluminum. Finally, the micron-sized aluminum powder was vaporized and burnt to release energy.

Figure 13 shows the reaction mechanism diagram of the micro-nano composite aluminum powder. Figure 13 indicates that nano aluminum has a great contribution to micron-sized aluminum combustion. Nano aluminum combustion will raise the temperature during the reaction of micron-sized aluminum, and with a more uniform distribution of nano aluminum, the reaction degree of the micron-sized aluminum powder was higher. Fluororubber plays an important part in the dispersion of aluminum powder. Without fluororubber, these aluminum powders will agglomerate and have a lower reaction degree. This is bad for the energy release of aluminum powder and an aluminum powder coated with fluororubber could solve this problem effectively.

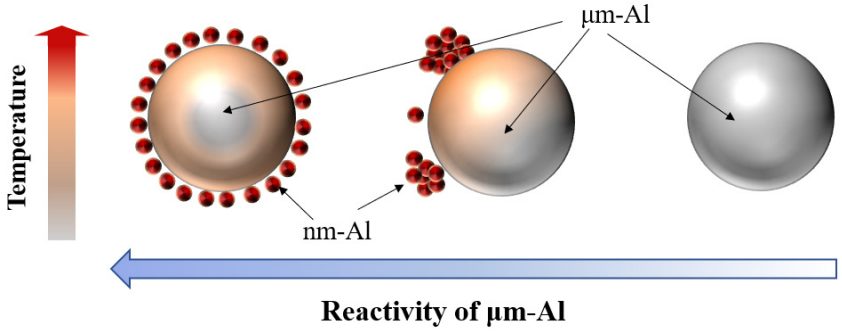

Figure 13. The reaction mechanism diagram of the micro-nano composite aluminum powder.

4. Conclusions

In this study, a special structure of aluminum powder was prepared by in situ electrical explosion. By means of characterization such as structure and composition analysis as well as combustion performance analysis such as constant volume combustion and laser ignition, combined with TG-DSC and numerical simulation, the combustion decomposition process of this micro-nano composite aluminum powder was studied and the following conclusions were obtained:

(1) In situ electrical explosion enabled the preparation of micro-nano composite structures with a mixture of nano- and micron-sizes, and by observing this, the nano-sized aluminum was dispersed on micron-sized aluminum spheres, so the structure exhibited a sea urchin structure.

(2) By adding a fluororubber, the surface of the micro-nano composite structure was covered with a layer of a gas-producing substance, which will benefit the dispersion and combustion of aluminum powder.

(3) The results of the heat transfer calculations show that the combustion of nano aluminum powder will increase the participation temperature of micron-sized aluminum powder in the reaction. Then, the micron-sized aluminum powder will release energy more rapidly and completely. The combustion time of the micron-sized aluminum and the micro-nano composite aluminum was 9.603 μs and 3.873 μs, separately. This micro-nano composite aluminum powder will provide a favorable reference for the application of aluminum powder in the field of explosives and propellants.

Author Contributions: Conceptualization, X.W. and H.R.; Methodology, X.W.; Software, X.W.; Validation, X.W., H.R. and Q.J.; Formal analysis, X.W.; Investigation, X.W.; Resources, H.R.; Data curation, Q.J.; Writing—original draft preparation, X.W.; Writing—review and editing, H.R.; Visualization, X.W.; Supervision, H.R.; Project administration, H.R.; Funding acquisition, H.R. and Q.J. All authors have read and agreed to the published version of the manuscript.

Funding: This research was funded by the National Natural Science Foundation of China (grant number 21975024).

Data Availability Statement: The data presented in this study are presented in the figures and tables in this article.

Acknowledgments: We thank SiChuan Hbst. Co., Ltd., China for the materials used in the experiments.

Conflicts of Interest: The authors declare no conflict of interest.

References

1. Yin, H.Q.; Pan, Q.; Zhang, J.L.; Wang, G.Z.; Yang, Q.S. The Influence of Aluminum Powder on Explosive Performance. *Energetic Mater.* **2004**, *5*, 318–320+256.
2. Makhov, M.N. Acceleration Ability of Aluminum-Containing Explosive Compositions. *Russ. J. Phys. Chem. B* **2018**, *12*, 258–265. [CrossRef]
3. Ermolaev, B.S.; Khasainov, B.A.; Baudin, G.; Presles, A.N. Behavior of aluminum in detonation of high explosives. Surprises and interpretations. *Chem. Phys. Rep.* **2000**, *18*, 1121–1140.
4. Dong, J.; Wang, W.L.; Wang, X.F.; Zhou, Q.; Miao, R.; Du, M.H.; Tan, B.; Wang, Y.J.; Zhang, T.Y.; Li, Y.F.; et al. Effects of Nano Aluminum Powder on the Mechanical Sensitivity of RDX-Based Explosives. *Nanomaterials* **2021**, *11*, 2182. [CrossRef] [PubMed]
5. Li, Y.Y.; Wang, X.F.; Niu, Y.L.; Xiao, Q.; Li, X. Reaction rate of Al powder in different explosion atmosphere. *Sci. Technol. Eng.* **2020**, *20*, 2700–2704.
6. Miao, S.Q.; Xu, G.G.; Wang, T.Z. Mechanism analysis of the influence of Al shape and size on the detonation properties of aluminized explosives. *Chin. J. Explos. Propellants* **2002**, *25*, 4–5.
7. Feng, X.J.; Huang, Y.F.; Xu, H.T. The influence of Al on the detonation parameters of Aluminized explosives. *Initiat. Pyrotech.* **2012**, *1*, 38–41.
8. Feng, X.S.; Feng, X.J.; Zhao, J.; Tian, X. Effect of content and particle size of aluminum powder on the air blast property of HMX-based explosive. *Explos. Mater.* **2018**, *47*, 10–15.
9. Sundaram, D.S.; Puri, P.; Yang, V. A general theory of ignition and combustion of nano- and micron-sized aluminum particles. *Combust. Flame* **2016**, *169*, 94–109. [CrossRef]
10. Sundaram, D.S.; Yang, V.; Zarko, V.E. Combustion of nano aluminum particles (Review). *Combust. Explos. Shock Waves* **2015**, *51*, 173–196. [CrossRef]

11. Storozhev, V.B.; Yermakov, A.N. Combustion of nano-sized aluminum particles in steam: Numerical modeling. *Combust. Flame* **2015**, *162*, 4129–4137. [CrossRef]
12. Niu, G.T.; Cao, S.T.; Niu, L.; Jin, D.Y.; Yao, L.N. Dispersibility and formability of explosives with nano-aluminum. *Sci. Technol. Eng.* **2021**, *21*, 8018–8022.
13. Woody, D.L.; Dokhan, A.; Johnson, C.E. Performance comparisons of nanoaluminum, coated microaluminum and their bimodal mixtures. In Proceedings of the 13th Conference of the American-Physical-Society-Topical-Group on Shock Compression of Condensed Matter, Portland, OR, USA, 20–25 July 2003; pp. 906–909.
14. Jiang, F.; Wang, X.F.; Huang, Y.F.; Feng, B.; Tian, X.; Niu, Y.L.; Zhang, K. Effect of particle gradation of aluminum on the explosion field pressure and temperature of RDX-based explosives in vacuum and air atmosphere. *Def. Technol.* **2019**, *15*, 844–852. [CrossRef]
15. Moore, K.; Pantoya, M.L.; Son, S.F. Combustion behaviors resulting from bimodal aluminum size distributions in thermites. *J. Propuls. Power* **2007**, *23*, 181–185. [CrossRef]
16. McCollum, J.M.; Pantoya, M.L.; Iacono, S.T. Activating Aluminum Reactivity with Fluoropolymer Coatings for Improved Energetic Composite Combustion. *ACS Appl. Mater. Interfaces* **2015**, *7*, 18742–18749. [CrossRef]
17. Kim, D.W.; Kim, K.T.; Min, T.S.; Kim, K.J.; Kim, S.H. Improved Energetic-Behaviors of Spontaneously Surface-Mediated Al Particles. *Sci. Rep.* **2017**, *7*, 4659. [CrossRef]
18. Sippel, T.R.; Son, S.F.; Groven, L.J. Aluminum agglomeration reduction in a composite propellant using tailored Al/PTFE particles. *Combust. Flame* **2014**, *161*, 311–321. [CrossRef]
19. Sindhu, T.K.; Sarathi, R.; Chakravarthy, S.R. Understanding nanoparticle formation by a wire explosion process through experimental and modelling studies. *Nanotechnology* **2008**, *19*, 025703. [CrossRef]
20. Neelmani; Rengaswamy, J.; Raghuraman, C.S.; Hisayuki, S.; Ramanujam, S. Enhancement of hydrogen generation using nanoaluminum particles produced by a wire explosion process. *IEEJ Trans. Electr. Electron. Eng.* **2019**, *14*, 810–818. [CrossRef]
21. Nazarenko, O.B.; Amelkovich, Y.A.; Sechin, A.I. Characterization of aluminum nanopowders after long-term storage. *Appl. Surf. Sci.* **2014**, *321*, 475–480. [CrossRef]
22. Lerner, M.I.; Glazkova, E.A.; Lozhkomoev, A.S.; Svarovskaya, N.V.; Bakina, O.V.; Pervikov, A.V.; Psakhie, S.G. Synthesis of Al nanoparticles and Al/AlN composite nanoparticles by electrical explosion of aluminum wires in argon and nitrogen. *Powder Technol.* **2016**, *295*, 307–314. [CrossRef]
23. Kissinger, H.E. Reaction Kinetics in Differential Thermal Analysis. *Anal. Chem.* **1957**, *29*, 1702–1706. [CrossRef]
24. Ozawa, T. Kinetic analysis of derivative curves in thermal analysis. *J. Therm. Anal.* **1970**, *2*, 301–324. [CrossRef]
25. Ozawa, T. A New Method of Analyzing Thermogravimetric Data. *Bull. Chem. Soc. Jpn.* **1965**, *38*, 1881–1886. [CrossRef]
26. Wang, J.; Yang, H.T.; Cheng, L.; Gao, P.; Li, Y.C.; Song, D.M. Ignition and Combustion Characteristics of B/NC/CuO Thermite Microparticles. *Metals* **2022**, *12*, 1419. [CrossRef]
27. Yao, J.; Huang, Y.J.; Chang, K.H.; Nie, J.X.; Guo, X.Y.; Shen, C.; Yan, S. Preparation and Energy Release Properties of nB@F2603@CL-20 Microspheres by Electrospray. *Metals* **2022**, *12*, 1727. [CrossRef]
28. An, Y.J.; Zhu, L.; Jin, S.H.; Lu, J.J.; Liu, X.Y. Laser-Ignited Self-Propagating Sintering of AlCrFeNiSi High-Entropy Alloys: An Improved Technique for Preparing High-Entropy Alloys. *Metals* **2019**, *9*, 438. [CrossRef]
29. Riello, D.; Zetterstrom, C.; Parr, C.; Braulio, M.A.L.; Moreira, M.; Gallo, J.B.; Pandolfelli, V.C. AlF_3 reaction mechanism and its influence on alpha-Al_2O_3 mineralization. *Ceram. Int.* **2016**, *42*, 9804–9814. [CrossRef]
30. Nie, J.X.; Kan, R.Z.; Jiao, Q.J.; Wang, Q.S.; Guo, X.Y.; Yan, S. Studies on aluminum powder combustion in detonation environment. *Chin. Phys. B* **2022**, *31*, 044703. [CrossRef]